THE JOURNAL OF BIOLOGICAL CHEMISTRY
Vol. 279, No. 24, Issue of June 11, pp. 25219–25225, 2004

Printed in U.S.A.

Arachidonic Acid Released by Phospholipase A_2 Activation Triggers Ca^{2+}-dependent Apoptosis through the Mitochondrial Pathway*

Received for publication, September 18, 2003, and in revised form, February 27, 2004
Published, JBC Papers in Press, April 7, 2004, DOI 10.1074/jbc.M310381200

Daniele Penzo‡§¶, Valeria Petronilli‡, Alessia Angelin‡, Claudia Cusan‖, Raffaele Colonna‡, Luca Scorrano§, Francesco Pagano§, Maurizio Prato‖, Fabio Di Lisa‡‡, and Paolo Bernardi‡§ §§**

From the Departments of ‡Biomedical Sciences and ‡‡Biological Chemistry, Consiglio Nazionale delle Ricerche Institute of Neuroscience at the University of Padova, Viale Giuseppe Colombo 3, I-35121 Padova, Italy, the ‖Department of Pharmaceutical Sciences, University of Trieste, Piazzale Europa 1, I-34127 Trieste, Italy, and the §Dulbecco-Telethon Institute at the Venetian Institute of Molecular Medicine, Via Orus 2, I-35129 Padova, Italy

We studied the effects of the divalent cation ionophore A23187 on apoptotic signaling in MH1C1 cells. Addition of A23187 caused a fast rise of cytosolic Ca^{2+} ($[Ca^{2+}]_c$), which returned close to the resting level within about 40 s. The $[Ca^{2+}]_c$ rise was immediately followed by phospholipid hydrolysis, which could be inhibited by aristolochic acid or by pretreatment with thapsigargin in Ca^{2+}-free medium, indicating that the Ca^{2+}-dependent cytosolic phospholipase A_2 ($cPLA_2$) was involved. These early events were followed by opening of the mitochondrial permeability transition pore (PTP) and by apoptosis in about 30% of the cell population. In keeping with a cause-effect relationship between addition of A23187, activation of $cPLA_2$, PTP opening, and cell death, all events but the $[Ca^{2+}]_c$ rise were prevented by aristolochic acid. The number of cells killed by A23187 was doubled by treatment with 0.5 μM MK886 and 5 μM indomethacin, which inhibit arachidonic acid metabolism through the 5-lipoxygenase and cyclooxygenase pathway, respectively. Consistent with the key role of free arachidonic acid, its levels increased within minutes of treatment with A23187; the increase being more pronounced in the presence of MK886 plus indomethacin. Cell death was preceded by cytochrome *c* release and cleavage of caspase 9 and 3, but not of caspase 8. All these events were prevented by aristolochic acid and by the PTP inhibitor cyclosporin A. Thus, A23187 triggers the apoptotic cascade through the release of arachidonic acid by $cPLA_2$ in a process that is amplified when transformation of arachidonic acid into prostaglandins and leukotrienes is inhibited. These findings identify arachidonic acid as the causal link between A23187-dependent perturbation of Ca^{2+} homeostasis and the effector mechanisms of cell death.

Regulation of cell death by Ca^{2+} is a problem of great complexity. First proposed in the early 1970s as a mediator of cell demise in heart ischemia (1, 2), Ca^{2+} is today considered a key to both necrosis and apoptosis through its modulation of transcriptional factors, kinase and phosphatase signaling cascades, activation of enzymes involved in protein degradation and phospholipid metabolism, and modulation of mitochondrial function (3).

Mitochondria are central to Ca^{2+} signaling. This is true of both the response to physiological stimuli that pertains to normal cell function and the response to apoptotic signals that leads to cell demise (4). A key switch between cell survival and cell death is the mitochondrial PTP,[1] a high conductance channel that may open in response to mitochondrial Ca^{2+} uptake (5). The PTP participates in the release of proapoptotic proteins through at least two mechanisms: swelling-dependent rupture of the outer mitochondrial membrane and remodeling of mitochondrial cristae, which increases the availability of cytochrome *c* for release through specific pathways activated by outer membrane tBID insertion (6, 7). PTP opening is not always followed by cell death, and the relationship between the two events appears to correlate with the pore open time. Only openings that last long enough to cause measurable depolarization are followed by cytochrome *c* release and detrimental effects on cell survival (8, 9).

A key aspect of PTP pathophysiology is that matrix Ca^{2+} is an essential permissive factor for pore opening, yet Ca^{2+} alone may not be sufficient. Indeed, only under conditions of overload, Ca^{2+} as such can trigger PTP opening in isolated mitochondria, an event that is also facilitated by the accompanying matrix alkalinization (10). Under the conditions prevailing *in situ*, the PTP open-closed transitions are modulated by a large variety of additional factors that may critically affect the outcome of an identical Ca^{2+} signal (5). Many apoptotic signaling molecules act as PTP inducers, and these include lipid mediators like ceramides (11, 12), GD3 ganglioside (13–16), and arachidonic acid (17–19). The latter is particularly interesting in the context of Ca^{2+}-dependent cell death. Indeed, it has been shown that arachidonic acid-selective, Ca^{2+}-dependent $cPLA_2$ is essential for the cytotoxic action of tumor necrosis factor α (20), which triggers PTP opening (21) through activation of phospholipid hydrolysis (17) and that arachidonic acid signals apoptosis (22, 23) through a mitochondrial effect that can be amplified by inhibition of LOX and COX (18).

* This work was supported in part by Grants from the Associazione Italiana per la Ricerca sul Cancro and the Ministero per l'Università e la Ricerca Scientifica e Tecnologica. The costs of publication of this article were defrayed in part by the payment of page charges. This article must therefore be hereby marked "*advertisement*" in accordance with 18 U.S.C. Section 1734 solely to indicate this fact.

¶ Submitted in partial fulfillment of the requirements for a Ph.D. at the University of Padova.

** Recipient of Grant TCP 02016 from Telethon-Italy.

§§ To whom correspondence should be addressed: Dept. of Biomedical Sciences, University of Padova, Viale Giuseppe Colombo 3, I-35121 Padova, Italy. Fax: 39-049-827-6361; E-mail: bernardi@bio.unipd.it.

[1] The abbreviations used are: PTP, permeability transition pore; bis-BODIPY®-FL-C_{11}-PC, 1,2-bis-(4,4-difluoro-5,7-dimethyl-4-bora-3a,4a-diaza-s-indacene-3-undecanoyl)-*sn*-glycero-3-phosphocholine; $[Ca^{2+}]_c$, cytosolic Ca^{2+} concentration; COX, cyclooxygenase; $cPLA_2$, cytosolic phospholipase A_2; CsA, cyclosporin A; HBSS, Hanks' balanced salt solution; LOX, lipoxygenase; MH1C1, Morris Hepatoma of the rat clone 1C1; MK886, 3-[3-*tert*-butylsulfanyl-1-(4-chlorobenzyl)-5-isopropyl-*1H*-in-dol-2-yl]-2,2-dimethylpropionic acid; HETE, hydroxyeicosatetraenoic acid; AM, acetomethoxy ester.

Addition of A23187 should allow Ca^{2+} equilibration with an increase of $[Ca^{2+}]_c$, which should mimic the Ca^{2+} overload taking place under pathological conditions at proper concentrations and incubation times (24–31). Unexpectedly, however, we found that addition of A23187 to MH1C1 cells caused a slow mitochondrial depolarization and death of about 30% of cells, findings that are inconsistent with the expected consequences of cellular Ca^{2+} overload (9). Here we show that addition of A23187 caused a fast but only transient rise of $[Ca^{2+}]_c$, which was sequentially followed by a rapid increase of cPLA$_2$ activity and then by PTP opening, the latter event occurring when $[Ca^{2+}]_c$ had already returned to nearly basal levels. We identified the proapoptotic signal triggered by A23187 as free arachidonic acid, whose levels could be dramatically increased by treatment with the LOX inhibitor MK886 plus the COX inhibitor indomethacin. A23187-triggered cell death was preceded by PTP opening, cytochrome *c* release, and cleavage of caspase 9 and 3, but not of caspase 8. All these events except for the transient rise of $[Ca^{2+}]_c$ were blocked by the cPLA$_2$ inhibitor aristolochic acid or by the PTP inhibitor CsA. Thus, the major effect of the $[Ca^{2+}]_c$ increase caused by A23187 is activation of cPLA$_2$ with generation of arachidonic acid, which causes apoptosis exclusively through the mitochondrial pathway. This signaling pathway is amplified when transformation of arachidonic acid into prostaglandins and leukotrienes has been inhibited.

EXPERIMENTAL PROCEDURES

Cell Cultures—MH1C1 cells were grown in Ham's F-10 nutrient mixture supplemented with 10% fetal calf serum in a humidified atmosphere of 95% air, 5% CO_2 at 37 °C in a Forma tissue culture water-jacketed incubator. For experiments of fluorescence microscopy, cells were seeded onto uncoated 24-mm (for calcein, fluo-3, bis-BODIPY®-FL-C_{11}-PC, and annexin V staining) or 13-mm (for immunofluorescence) diameter round glass coverslips (50,000 cells/coverslip) and grown for 2 days as described above.

Fluo-3 Staining and Imaging—Cells were loaded with 5 μM fluo-3-AM (acetomethoxy ester) for 1 h at 37 °C in 1 ml of bicarbonate- and phenol red-free HBSS supplemented with 10 mM Hepes, pH 7.4, 0.005% pluronic acid, and 2 μM cyclosporin H (CsH) (32). Cells were then washed free of fluo-3 and pluronic acid and maintained in HBSS-Hepes containing 2 μM CsH. Cellular fluorescence images were acquired with an Olympus IMT-2 inverted microscope, equipped with a xenon light source (75 watts) for epifluorescence illumination and with a 12-bit digital-cooled CCD camera (Micromax, Princeton Instruments). For detection of fluorescence, 488 ± 25 nm excitation and 525-nm longpass emission filter settings were used. Images were collected with exposure times ranging between 50 and 100 ms using a ×10 objective (Nikon). Data were acquired and analyzed using Metamorph software (Universal Imaging). Whole cells were identified as regions of interest, and fields not containing cells were taken as the background. Unless otherwise stated, sequential digital images were acquired every minute, and the average fluorescence intensity of all relevant regions was recorded and stored for subsequent analysis. The maximal fluo-3 fluorescence signal at saturating $[Ca^{2+}]_c$ was obtained by adding 5 μM digitonin at the end of each experiment, and cell fluorescence intensities minus background are reported in the figures after normalization of the maximal fluorescence for comparative purposes.

Calcein Staining and Imaging—Cells were loaded with 2 μM calcein-acetomethoxy ester (Molecular Probes, Eugene, OR) for 30 min at 37 °C in 1 ml of HBSS-Hepes pH 7.4 and 1 mM $CoCl_2$ (Sigma) (8). Cells were then washed free of calcein and Co^{2+} and maintained in HBSS-Hepes. When specified, 2 μM CsA (Fluka Riedel-de Haen) or 50 μM aristolochic acid (Alexis Biochemicals) were added to the cells after probe loading, and fluorescence acquisition was started 30 min later. Cellular fluorescence images were acquired with the Olympus IMT-2 microscope with the same settings described above for fluo-3. Images were collected with exposure times ranging between 50 and 100 ms using a ×40, 1.3 numerical aperture (NA) oil immersion objective (Nikon). Data were acquired and analyzed using Metamorph software. Clusters of several mitochondria (10–30) were identified as regions of interest, and fields not containing cells were taken as the background. Sequential digital images were acquired every 60 s, and the average fluorescence intensity of all relevant regions was recorded and stored for subsequent analysis. Mitochondrial fluorescence intensities minus background are reported in the figures after normalization of the initial fluorescence for comparative purposes, and they represent the mean of 10 regions of interest.

Loading and Cleavage of bis-BODIPY®-FL-C_{11}-PC—Loading of MH1C1 cells with bis-BODIPY®-FL-C_{11}-PC (a synthetic phospholipid containing fluorescein in position 2 that is dequenched upon cleavage) was performed as in Ref. 17 except that the molar ratio of dipalmitoylphosphatidyl-serine (Sigma), cholesterol (Sigma), and bis-BODIPY®-FL-C_{11}-PC (Molecular Probes) in liposomes was 1:6:15. After washing twice with HBSS-Hepes, cells were incubated for 30 min at 37 °C as specified in the legend to Fig. 2 and then imaged as described below. Fluorescence images were acquired with a Nikon Eclipse TE200 inverted microscope equipped with a mercury light source for epifluorescence illumination, with a cooled digital CCD camera, and with a PerkinElmer Ultraview LCI confocal imaging system 4.0 volume wizard 1.1. Filter settings were 480 ± 25 nm excitation and 525-nm longpass emission, and images were collected every 5 s with an exposure time of 500 ms using a ×60, 1.3 NA oil immersion objective (Nikon). Data were acquired and analyzed using Metamorph software. Sequential digital images were acquired at the times indicated in Fig. 2, and the total fluorescence of 10 cells in each field was recorded and stored. The data were corrected for background fluorescence, and initial fluorescence values are normalized for comparative purposes.

Lipid Analysis—Cells were treated with A23187 and other reagents as specified in the legend to Figs. 8 and 9, and then extracted with chloroform/methanol exactly as described in Ref. 33 except that homogenization was carried out on ice for 15 min, and the sample was not filtered. The lipid extracts were subjected to thin layer chromatography on 10 × 10 cm plates (Merck, Darmstadt n. 5641) as specified in the figure legends, and the migration of specific lipids was identified with authentic standards (Avanti polar lipids). The plates were sprayed with 20% (v/v) H_2SO_4, and the spots were visualized by heating.

Gas Chromatography and Mass Spectrum Analysis—Cell extracts were taken to complete dryness with a gentle stream of N_2 gas and then 10 μl of $CHCl_3$ were added to give a homogeneous solution, and 1 μl was injected in the gas chromatograph. Analysis was carried out with a Finningan MAT GCQ (EI ion mode positive) mass spectrometer interfaced to a Finningan MAT gas chromatograph equipped with a CP-Sil 8 CB LOW BLEED/MS column, 30 m × 0.25 mm, film thickness 0.25 μm, WCOT fused-silica capillary column. The temperature of the column oven was kept at 100 °C for 10 min and then increased from 100 to 300 °C at a rate of 10 °C per min^{-1}. Once the temperature of 300 °C had been reached, it was maintained for 1 min. The temperatures of the injection port and the transfer line were maintained at 180 and 275 °C, respectively, and that of the ion source at 200 °C. The ionization energy and the trap current were 70 eV and 250 μA, respectively, and helium was used as the carrier gas. Full scan mass spectra were acquired by scanning from *m/z* 50 to 400 with a scan time of 1 s.

Cytochrome c Release and Cell Death—For staining with annexin V, each coverslip was incubated for 15 min at 25 °C in 0.5 ml of a solution containing 140 mM NaCl, 5 mM $CaCl_2$, and 10 mM Hepes-NaOH, pH 7.4, 2 μM propidium iodide (Sigma) and annexin V-FLUOS (Roche Applied Science) to a final dilution of 1:25 (v/v). Cells were washed twice with HBSS-Hepes before analysis. Cellular fluorescence images were acquired the Olympus IMT-2 inverted microscope exactly as described (13). Immunodetection of the relative distribution of the bc_1 complex and of cytochrome *c* was carried out and analyzed as described in Ref. 9. The analysis yields a "localization index" of 1 when the distribution of cytochrome *c* matches that of the bc_1 complex, whereas the index decreases as the distribution of cytochrome *c* becomes more diffuse (9).

Caspase Cleavage—MH1C1 cells were grown to near confluence in 25-cm^2 tissue culture flasks. The flasks were rinsed with serum-free medium, and the cells were further treated as described in the legends to Figs. 6 and 7. Because the various treatments led to detachment of a variable proportion of cells, at the end of the experiment the medium with floating cells was removed from each flask and transferred to individual polypropylene test tubes for subsequent pooling with the adherent cells from the same flask. The flasks were then rinsed with phosphate-buffered saline and treated with 0.5 ml of trypsin (0.05%, w/v) plus EDTA (0.02%, w/v) for 2 min. Following the addition of 4.5 ml of serum-free medium, cells were withdrawn, pooled with the medium previously removed from each flask, and collected by centrifugation at 1,000 × *g* for 5 min. The supernatants were carefully removed, and each pellet was dissolved in 1 ml of ice-cold lysis buffer (150 mM NaCl, 50 mM Tris-HCl, pH 7.5, 1% Nonidet P-40, 1 μg ml^{-1} phenylmethylsulfonyl fluoride, 1 μg ml^{-1} pepstatin, and 1 μg ml^{-1} leupeptin). After 30 min at 4 °C, the extracts were cleared by centrifugation at 14,000 × *g* at 4 °C

for 10 min. The protein concentration of each extract was determined with the Bradford reagents (Bio-Rad), and equal protein amounts were precipitated with 4 volumes of ice-cold acetone for 10 min followed by centrifugation at 14,000 × *g*. The acetone was removed, the samples were air-dried at room temperature, and the pellets were finally dissolved by boiling for 5 min in Laemmli gel sample buffer containing 5% 2-mercaptoethanol. Proteins were resolved by SDS-PAGE on 1.5-mm thick 12% acrylamide-0.4% bisacrylamide minigels, transferred to nitrocellulose, and probed with antibodies against caspases 8 and 9 (Santa Cruz Biotechnology), and 3 (Cell Signaling; they all recognized both the uncleaved and cleaved forms of caspases). Treatment of MH1C1 cells with 2 μg ml^{-1} of Fas ligand (Bender Chemicals) or 2 μM staurosporine was used as a positive control for caspase 8 and caspase 9 plus 3 cleavage, respectively.

Reagents—Other reagents include secondary peroxidase-conjugated antibodies from Southern Biotechnology and the peroxidase detection kit from Pierce. All other chemicals and tissue culture reagents were purchased from Sigma and were of the highest available grade.

RESULTS

Effects of A23187 on Intracellular Ca^{2+} Homeostasis—We investigated the effects of A23187 on $[Ca^{2+}]_c$ as measured from the fluorescence changes of fluo-3 in MH1C1 cells. Fig. 1 shows that the addition of 2 μM A23187 caused a fast fluorescence increase. The peak rise was nearly as high as that caused by the subsequent addition of a low concentration of digitonin, used here to determine the maximal fluo-3 signal at saturating $[Ca^{2+}]_c$ (*trace a*). The increase of $[Ca^{2+}]_c$ was transient, with a return of the fluorescence to a level slightly higher than the initial value within about 40 s of the addition of A23187 (*inset, trace a*). The $[Ca^{2+}]_c$ transient induced by A23187 was reduced in height but not abolished by pretreatment with 2 μM thapsigargin for 30 min or by incubation in Ca^{2+}-free medium containing 0.1 mM EGTA (results not shown). However, it was completely blunted by a combination of the two treatments (Fig. 1, *trace b*). These findings indicate that both extracellular Ca^{2+} and intracellular Ca^{2+} stores contribute to the $[Ca^{2+}]_c$ transient induced by A23187. The $[Ca^{2+}]_c$ response depicted in Fig. 1 was observed in all treated cells, yet A23187 caused cell death only in about 30% of the population (9) (see also Fig. 4 below). Taken together, these findings suggest that the initial $[Ca^{2+}]_c$ rise may have generated additional signal(s) causing cell death in a subpopulation of sensitive cells.

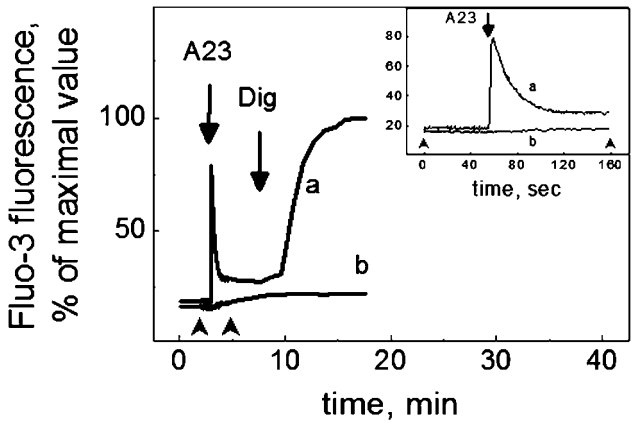

FIG. 1. **$[Ca^{2+}]_c$ transients induced by A23187 in MH1C1 cells.** MH1C1 cells were loaded with fluo-3-AM as described under "Experimental Procedures," and images were collected every minute except during the time frame delimited by the *arrowheads*, when images were collected every 500 ms. Where indicated (*arrows*) 2 μM A23187 (*A23*) was added, followed by 5 μM digitonin (*Dig*) in *trace a* only. *Trace a* was obtained from an individual cell incubated in a Ca^{2+}-competent medium, whereas *trace b* was recorded from a cell preincubated for 30 min with 2 μM thapsigargin in a nominally Ca^{2+}-free medium containing 0.1 mM EGTA. The maximal fluo-3 fluorescence for the experiment of *trace b* was obtained by adding 1.2 mM Ca^{2+} followed by 5 μM digitonin (results not shown for clarity). *Inset*, fluorescence changes induced by A23187 are shown with an expanded time scale. The experiments are representative of ten replicates.

Effects of A23187 on Phospholipid Hydrolysis and PTP Opening—We next investigated whether A23187 could initiate early phospholipid hydrolysis. To this end, cells were enriched with the synthetic phospholipid bis-BODIPY®-FL-C$_{11}$-PC, which undergoes dequenching (with a corresponding fluorescence increase) upon cleavage of the labeled phospholipid in position 2. It can be seen that the addition of 2 μM A23187 caused a mostly intracellular fluorescence increase (Fig. 2, *panel B*), in keeping with the recent demonstration that cPLA$_2$ translocates to intracellular membranes after its activation (34–37). Consistent with activation of the Ca^{2+}-dependent cPLA$_2$, phospholipid hydrolysis triggered by A23187 was inhibited by aristolochic acid (38–40) or by treatment with thapsigargin in the presence of EGTA, but not by the PTP inhibitor CsA (Fig. 2, *panel C*). Note that the process of phospholipid hydrolysis detected by bis-BODIPY®-FL-C$_{11}$-PC immediately followed the $[Ca^{2+}]_c$ rise induced by A23187 (Fig. 2, *panel C*, compare with the *inset* in Fig. 1). It must be stressed that neither aristolochic acid nor CsA modified the extent or kinetics of the $[Ca^{2+}]_c$ response to A23187 (results not shown).

We have previously shown that treatment of MH1C1 cells with tumor necrosis factor α activates phospholipid hydrolysis followed by PTP opening (17). We tested whether PLA$_2$ activation by A23187 caused PTP opening with the sensitive calcein loading Co^{2+}-quenching technique (8). The experiments shown in Fig. 3, *panel A* show that treatment with 2 μM A23187 was

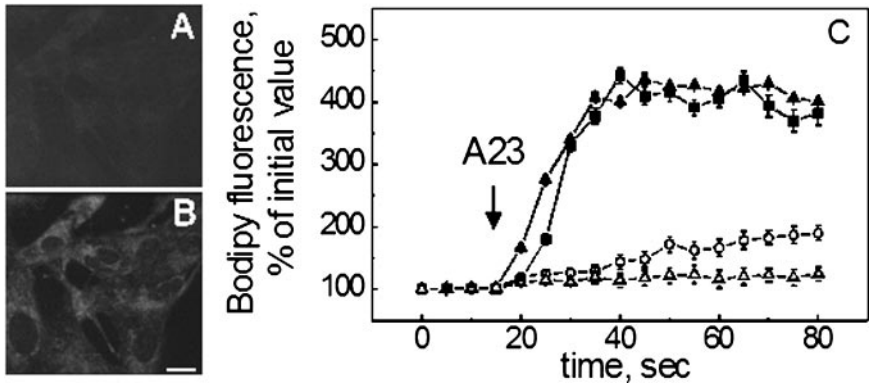

FIG. 2. **Effects of aristolochic acid and CsA on phospholipid hydrolysis induced by A23187.** MH1C1 cells were loaded with bis-BODIPY®-FL-C11-PC as described under "Experimental Procedures." *Panels A* and *B* show representative images taken before and 20 s after the addition of 2 μM A23187, respectively. *Panel C*, time course of whole cell fluorescence intensities minus background (mean values of 10 cells from three different experiments ± S.D.). Where indicated (*arrow*) 2 μM A23187 (*A23*) was added to control cells (*closed squares*); to cells that had been pretreated for 30 min with 50 μM aristolochic acid (*open circles*) or 2 μM CsA (*closed triangles*); or to cells that had been pretreated for 30 min with 2 μM thapsigargin in a nominally Ca^{2+}-free medium containing 0.1 mM EGTA (*open triangles*).

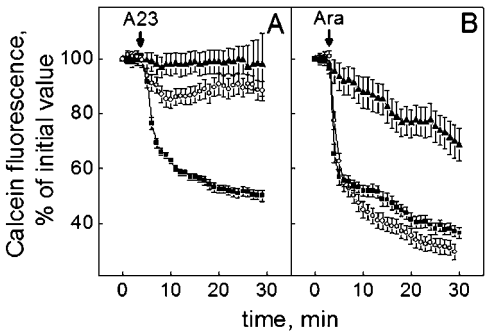

FIG. 3. **Effects of aristolochic acid and CsA on the mitochondrial calcein fluorescence changes induced by A23187 and arachidonic acid.** MH1C1 cells were co-loaded with calcein-AM and $CoCl_2$ as described under "Experimental Procedures," and images were collected at 60-s intervals. Where indicated (*arrows*) 2 μM A23187 (*A23*, *panel A*) or 75 μM arachidonic acid (*Ara*, *panel B*) were added to control cells (*closed squares*) or to cells that had been pretreated for 30 min with 50 μM aristolochic acid (*open circles*) or 2 μM CsA (*closed triangles*). The initial fluorescence intensities were normalized for comparative purposes, and values on the ordinate report the mean of four independent experiments ± S.D.

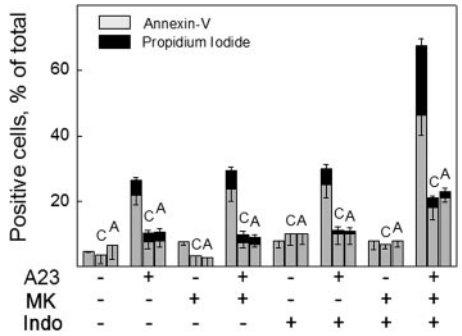

FIG. 4. **Cell death by A23187.** Stimulation by combined treatment with MK886 plus indomethacin and inhibition by CsA and aristolochic acid are shown. MH1C1 cells were grown on coverslips and treated for 5 h with vehicle (0.2%, v/v Me_2SO, first set of columns) or with 2 μM A23187 (*A23*), 0.5 μM MK886 (*MK*), and 5 μM indomethacin (*Indo*) where indicated by the (+) signs. The letters *C* and *A* denote incubations where 2 μM CsA or 50 μM aristolochic acid, respectively, were added 30 min before the treatment with A23187, MK886 and indomethacin. Cells were stained with annexin V-FLUOS and propidium iodide, and images were acquired as described under "Experimental Procedures." The fraction of annexin V-positive cells (*gray bars*) and double positive cells (*black bars*) was calculated from 20 randomly chosen fields from four independent experiments, and values are the mean ± S.D.

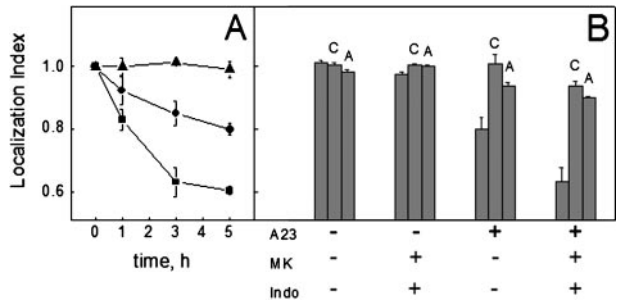

FIG. 5. **Cytochrome *c* release by A23187.** Stimulation by treatment with MK886 plus indomethacin and inhibition by CsA and aristolochic acid are shown. *Panel A*, MH1C1 cells were treated for the indicated times with vehicle (0.02% v/v Me_2SO, *triangles*), with 2 μM A23187 alone (*circles*), or with 2 μM A23187 (*A23*) after pretreatment with 0.5 μM MK886 (*MK*) and 5 μM indomethacin (*Indo*) for 30 min (*squares*). Cells were then fixed and treated with antibodies against the bc_1 complex and cytochrome *c*, and the localization index was determined exactly as described in Ref. 9. *Panel B*, MH1C1 cells were treated with vehicle or with 2 μM A23187 and/or 0.5 μM MK886 plus 5 μM indomethacin as indicated by the (+) signs. The letters *C* and *A* denote incubations where 2 μM CsA or 50 μM aristolochic acid, respectively, were added 30 min before the treatment with A23187 and MK886 plus indomethacin. After 3 h of incubation cells were fixed, and the localization index was determined as above. Values are mean ± S.D. of four (*panel A*) or three (*panel B*) different experiments.

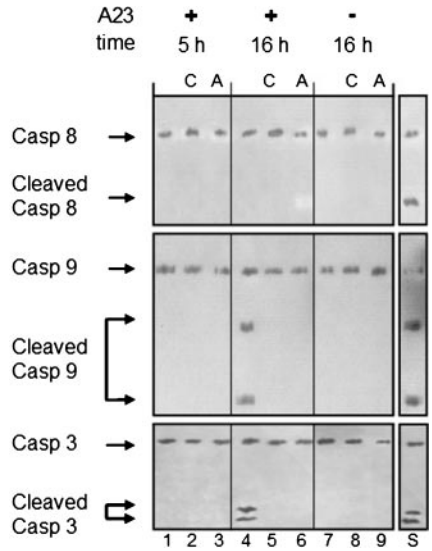

FIG. 6. **CsA- and aristolochic acid-sensitive cleavage of caspase 9 and 3, but not of caspase 8 by A23187.** MH1C1 cells in serum-free growth medium supplemented with 10 mM Hepes were treated with 2 μM A23187 (*A23*, *lanes 1–6*) or with vehicle (0.2% v/v Me_2SO, *lanes 7–9*). After the indicated times extracts prepared as described under "Experimental Procedures" were separated by SDS-PAGE (200 μg of protein in each lane), transferred to nitrocellulose, and probed with anti-caspase 8 (*upper panel*), anti-caspase 9 (*middle panel*), or anti-caspase 3 antibodies (*lower panel*). Letters *C* and *A* denote extracts prepared from incubations where 2 μM CsA or 50 μM aristolochic acid, respectively, were added to the flasks 30 min before the treatment with A23187 or vehicle. MH1C1 cells treated overnight with 2 μg ml^{-1} Fas ligand (*lane S*, *upper panel*) or 2 μM staurosporine (*lane S*, *lower panel*) were used as positive controls for caspase 8 and caspase 9 plus 3 cleavage, respectively. The position of uncleaved and cleaved caspases (*Casp*) is indicated by *arrows*.

readily followed by a decrease of mitochondrial calcein fluorescence (*closed squares*), which was expectedly (9) inhibited by CsA (*closed triangles*). The novel finding of Fig. 3 is that the PTP-inducing effects of A23187 could be inhibited by pretreatment with aristolochic acid (*open circles*). It must be stressed that the latter is not an inhibitor of the PTP. Indeed, Fig. 3 also shows that addition of arachidonic acid could bypass PTP inhibition by aristolochic acid (*panel B, open circles*) but not by CsA (*closed triangles*). These experiments establish a causal link between phospholipid hydrolysis and PTP opening in A23187-treated MH1C1 cells.

A23187 Induces Apoptosis through the Mitochondrial Pathway, Which Is Amplified by MK886 Plus Indomethacin—Despite the demonstrable increase of the PTP open time, Fig. 4 shows that A23187 caused the death of less than 30% of a population of MH1C1 cells within 5 h, see also Ref. 9. Cell killing was largely inhibited by aristolochic acid and CsA, indicating that phospholipid hydrolysis and PTP opening were involved in activation of the death program in a subpopulation of sensitive cells (Fig. 4). Because the cytotoxic effects of added arachidonic acid can be amplified by treatment with MK886 (a 5-LOX inhibitor) plus indomethacin (a general COX inhibitor) (18), we tested whether the fraction of cells responding with apoptosis to treatment with A23187 could be increased by MK886 and/or indomethacin. At the concentrations used in this study, neither MK886 nor indomethacin alone caused direct, short term toxicity to MH1C1 cells, nor did they increase the fraction of cells entering the apoptotic program upon stimula-

tion with A23187 (Fig. 4). When used in combination, however, MK886 and indomethacin increased the fraction of cells killed by A23187 to over 60%, in a process that maintained its sensitivity to both CsA and aristolochic acid (Fig. 4). It must be mentioned that neither MK886 nor indomethacin affected the $[Ca^{2+}]_c$ and bis-BODIPY®-FL-C_{11}-PC response to A23187 (results not shown).

To assess the pathway(s) for cell death we studied the kinetics of cytochrome *c* release and the pattern of caspase 8, 9, and 3 cleavage under the various conditions of the present study. A23187 induced release of cytochrome *c* that was potentiated by treatment with MK886 and indomethacin (Fig. 5, *panel A*) in a process that maintained its sensitivity to both aristolochic acid and CsA (Fig. 5, *panel B*). Consistent with selective activation of the mitochondrial pathway via cPLA$_2$ and the PTP: (i) A23187 caused cleavage of caspase 9 (Fig. 6, *middle panel*) and caspase 3 (Fig. 6, *lower panel*), which could be detected after 16 but not after 5 h of incubation (Fig. 6, compare *lane 4* with *lane 1*), but not of caspase 8 (Fig. 6, *upper panel*); (ii) in A23187-treated cells, MK886 plus indomethacin-potentiated cleavage of caspase 9 (Fig. 7, *middle panel*) and caspase 3 (Fig. 6, *lower panel*), which could be detected after 5 h of incubation (Fig. 7, compare *lane 10* with *lanes 4* and *7*), whereas cleavage of caspase 8 was not observed (Fig. 7, *upper panel*); (iii) both aristolochic acid (Figs. 6 and 7, *lanes* labeled *A*) and CsA (Figs. 6 and 7, *lanes* labeled *C*) fully prevented cleavage of caspases 9 and 3.

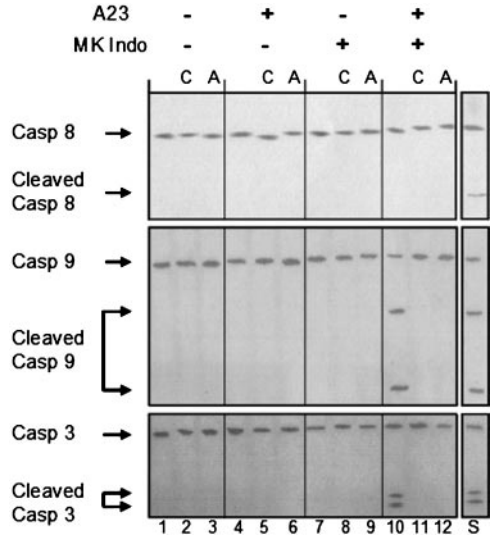

FIG. 7. **Combined treatment with MK886 and indomethacin amplifies the apoptotic effects of A23187.** MH1C1 cells in HBSS-Hepes buffer were treated for 5 h with vehicle (0.2% v/v Me_2SO, *lanes 1–3*) or with 2 μM A23187 (*A23*) and/or 0.5 μM MK886 plus 5 μM indomethacin (*MK Indo*) where indicated by the (+) signs. Cell extracts were prepared and probed exactly as described in the legend to Fig. 6. The letters *C* and *A*, and *lane S* have the same meaning as in Fig. 6.

A23187 Causes Accumulation of Free Arachidonic Acid in a Process Enhanced by MK886 Plus Indomethacin and Inhibited by Aristolochic Acid—Based on the pharmacological experiments reported so far (*i.e.* inhibition of cell death by aristolochic acid and its stimulation by MK886 and indomethacin) we hypothesized that the mechanism underlying A23187 toxicity was an increase of free arachidonic acid. To test this hypothesis, we studied the cellular lipid composition before and after treatment with A23187 by chloroform/methanol extraction followed by thin layer chromatography with chloroform (60%), methanol (30%), formic acid (7%), and H_2O (3%). The experiments of Fig. 8, *panel A* document that treatment with A23187 caused phospholipid hydrolysis, with appearance of lysophosphatidylcholine and lysophosphatidylethanolamine (the signal of lysophosphatidylserine could not be resolved from that of sphingomyelin). The lysophospholipids were detectable within 5 min of the addition of A23187 (*panel A*, *lane 2*), and their amount increased over the 30-min time frame of the experiment (*panel A*, *lanes 2–4*). Consistent with the experiments where phospholipid hydrolysis was followed with bis-BODIPY®-FL-C_{11}-PC (Fig. 2), formation of lysophospholipids was completely prevented by pretreatment with aristolochic acid (*panel A*, *lane* 6). An identical pattern of lysophospholipid formation was detected in cells pretreated with MK886 plus indomethacin (*panel A*, *lanes 7–11*). Analysis of the same samples with chloroform 95%, formic acid 5% as the eluent allowed resolution of the fatty acids, which accumulated with the same time course as the lysophospholipids after the addition of A23187 (*panel B*, *lanes 2* and *3*). Consistent with a key role of LOX and COX in fatty acid metabolism, the addition of MK886 and indomethacin greatly increased the amount of fatty acids detectable after treatment with A23187 (*panel B*, *lanes 7* and *8*). Finally, fatty acid production was completely blocked by aristolochic acid (*panel B*, *lanes 5* and *9*). The nature of the fatty acid(s) produced by phospholipid hydrolysis was determined by gas chromatography and mass spectroscopy of the lipid extracts. Only one species was detected after treatment

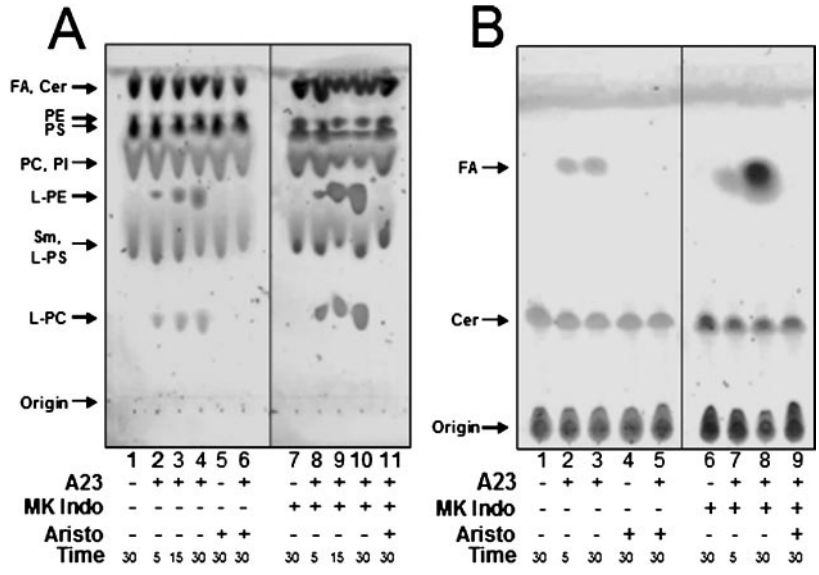

FIG. 8. **Effects of A23187, MK886, indomethacin, and aristolochic acid on the cellular lipid composition.** Where indicated by the (+) signs, cells were treated with 0.5 μM MK886 plus 5 μM indomethacin (*MK Indo*) and/or 50 μM aristolochic acid (*Aristo*), followed by the addition of 2 μM A23187 (*A23*). After the indicated times (min), cells were extracted with chloroform/methanol as described under "Experimental Methods," and lipids were separated by thin layer chromatography with chloroform/methanol/formic acid/water (60:30:7:3, v/v/v/v, *panel A*), or chloroform/formic acid (95:5, v/v, *panel B*). To determine the migration pattern of endogenous lipids authentic standards were used, and their position is indicated. *FA*, fatty acids; *Cer*, ceramide; *PE*, phosphatidylethanolamine; *PS*, phosphatidylserine; *PC*, phosphatidylcholine; *PI*, phosphatidylinositol; *L-PE*, lysophosphatidylethanolamine; *Sm*, sphingomyelin; *L-PS*, lysophosphatidylserine; *L-PC*, lysophosphatidylcholine.

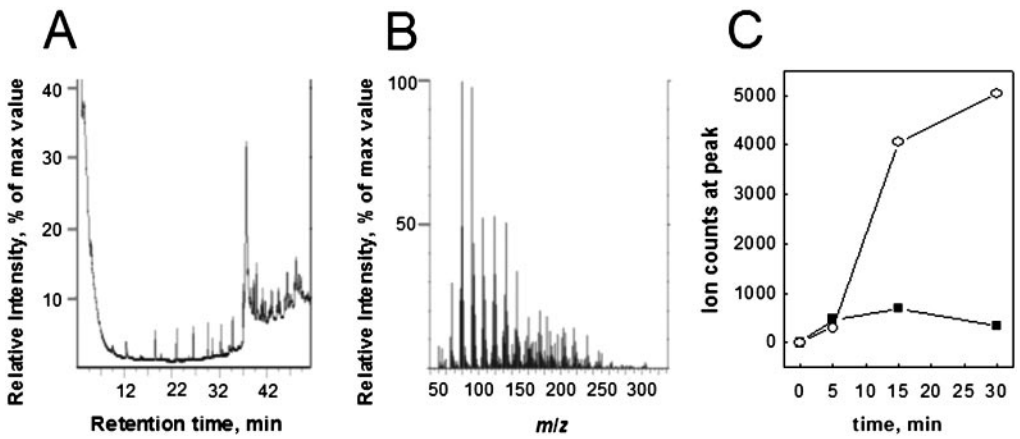

FIG. 9. **Identification of arachidonic acid as the product of phospholipid hydrolysis induced by A23187.** *Panel A*, a cellular extract prepared after 30 min of treatment with 2 μM A23187 in the presence of 0.5 μM MK886 plus 5 μM indomethacin was analyzed by gas chromatography. The sample was the same as that analyzed in Fig. 8, *panel B*, *lane 8*. *Panel B*, mass spectrum plot of the peak fraction from the gas chromatography, which eluted at the same retention time of authentic arachidonic acid. *Panel C*, time course of the free arachidonic acid increase in cells treated with 2 μM A23187 in the absence (*closed symbols*) or presence (*open symbols*) of 0.5 μM MK886 plus 5 μM indomethacin. The ion count (*y*-axis) was taken using the total ion current for the peak at 37 min (arachidonic acid) in the relative gas chromatogram.

with A23187 (Fig. 9, *panel A*), which had the same retention time as authentic arachidonic acid (not shown). The mass spectrum unequivocally identified the typical fragmentation pattern of arachidonic acid (304 *m/z*, 2%; 79, 100%; 91, 98%; 119, 55%; 147, 35%) (Fig. 9, *panel B*), and no other species could be detected throughout elution of the peak. A time course analysis revealed that upon addition of A23187 the peak concentration of arachidonic acid was reached at 15 min, with a decline at 30 min (Fig. 9, *panel C*). In the presence of MK886 plus indomethacin the concentration of arachidonic acid was about 10-fold higher, and continued to increase throughout the 30-min time course of the experiment (Fig. 9, *panel C*). Free arachidonic acid could still be detected in the extracts after 5 h of incubation with A23187 both in the absence and presence of MK886 plus indomethacin (results not shown).

DISCUSSION

The divalent cation ionophore A23187 was introduced in biomedical research in the early 1970s (41). It proved very useful to study mitochondrial ion transport (42, 43) and intracellular Ca^{2+} homeostasis (44), and as a tool to investigate Ca^{2+}-dependent processes like activation of cPLA$_2$ (45), arachidonic acid metabolism (46), and induction of cell death (24–31). Our work is generally consistent with previous reports on the cellular and mitochondrial effects of A23187 *in situ* (25–31), but it provides unique clues on the role of arachidonic acid released by cPLA$_2$ activation as the mechanistic link between A23187-dependent perturbation of Ca^{2+} homeostasis and the effector mechanisms of cell death.

The major findings of the present article are summarized in Fig. 10. We have established that a Ca^{2+}-dependent PLA$_2$ plays an essential role in the proapoptotic effects of A23187 in MH1C1 cells. Indeed, the rise of $[Ca^{2+}]_c$ that follows the addition of A23187 was transient; and it did not cause mitochondrial PTP opening and apoptosis as a direct consequence of Ca^{2+} overload. Rather, PTP opening, release of cytochrome *c*, activation of caspases 9 and 3, and cell death in a subset of sensitive cells were all initiated by hydrolysis of membrane phospholipids. It appears that the key enzyme involved in triggering these events is a phospholipase, the most likely candidate being cPLA$_2$ based on the following: (i) the inhibitory effects of aristolochic acid (38–40) and Ca^{2+} dependence (34) and (ii) the lack of expression of soluble PLA$_2$ in our cells (results not shown). Direct measurements have demonstrated that treatment with A23187 causes a selective increase of free

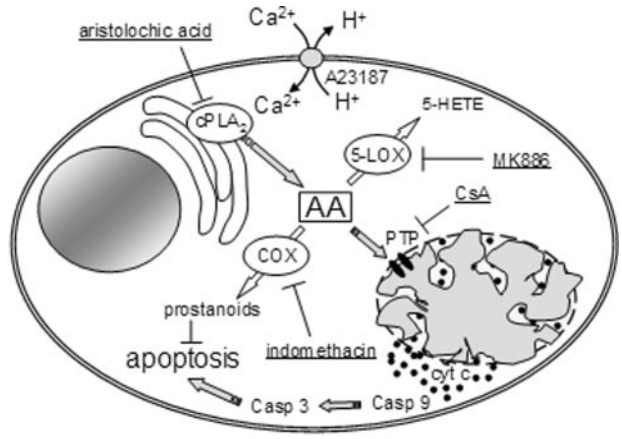

FIG. 10. **Schematic representation of the effects of A23187 and of the site of action of inhibitors.** Following activation of cPLA$_2$ by the transient $[Ca^{2+}]_c$ rise induced by A23187, arachidonic acid (*AA*) is released (although the effects of A23187 depend both on extracellular Ca^{2+} and on intracellular stores, only the former source is depicted for the sake of clarity). Arachidonic acid increases the open time of the PTP, which may result in release of cytochrome (*cyt c*) followed by activation of caspases (*Casp*) 9 and then 3. Arachidonic acid can be further metabolized by 5-LOX to generate 5-HETE, by COX to yield prostaglandins and related compounds, or enter other biosynthetic pathways that are not depicted here for clarity. Inhibition of 5-LOX with MK886 and of COX with indomethacin demonstrably increases the concentration of free arachidonic acid, potentiating its proapoptotic effects. Indomethacin would also promote apoptosis through inhibition of the synthesis of prostanoids, which generally have an antiapoptotic effect. Additional proapoptotic mediators acting on mitochondria could be generated from arachidonic acid, but this possible amplification loop has not been depicted in the scheme for simplicity. A23187-dependent apoptosis can be blocked upstream of arachidonic acid release by inhibition of cPLA$_2$ with aristolochic acid, or downstream of arachidonic acid release by PTP inhibition with CsA. Inhibitors used in the study are *underlined*; for further explanation see "Discussion."

arachidonic acid, which is further enhanced by the addition of MK886 (to inhibit 5-LOX) and indomethacin (to inhibit COX-1 and -2). The proapoptotic effects of A23187 are caused by the increase of free arachidonic rather than by the increase of $[Ca^{2+}]_c$ as such. Indeed, and irrespective of the presence of MK886 plus indomethacin, all the effects of A23187 (but Ca^{2+} rise) were blocked by aristolochic acid, and all the effects of A23187 (but Ca^{2+} rise and cPLA$_2$ activation) were blocked by the PTP inhibitor CsA. These findings fully support the scheme presented in Fig. 10, which highlights the key role of mitochon-

dria as downstream effectors of the apoptotic signal triggered by phospholipid hydrolysis and conveyed by arachidonic acid. It must be stressed that although arachidonic acid increases the PTP open time in isolated mitochondria (17), the effects of arachidonic acid released by cPLA$_2$ need not be caused by a direct action. Indeed, arachidonic acid also stimulates the hydrolysis of sphingomyelin and the generation of GD3 ganglioside, which could contribute in whole or in part to increase the PTP open time (11, 47–52).

Previous studies in cultured striatal neurons had shown that A23187-induced cell death was prevented by the caspase inhibitors acetyl-YVAD-CHO and acetyl-DEVD-CHO (29). These findings are consistent with an involvement of caspases, but they did not identify the specific caspases involved, and whether the caspase 8-dependent cleavage of BID was required to induce PTP opening and mitochondrial dysfunction. Our observation that caspases 9 and 3, but not caspase 8, were cleaved demonstrates that A23187-induced cell death entirely relies on the mitochondrial pathway.

A23187 has been widely used to study the role of Ca^{2+} in cell death (24–31). It is remarkable that, with few exceptions (*e.g.* Refs. 28, 30, and 31), the changes of $[Ca^{2+}]_c$ following the addition of A23187 have rarely been measured. Thus, the occurrence of Ca^{2+} overload following the addition of A23187 is often an explicit assumption (29), and the lack of information on the $[Ca^{2+}]_c$ changes in otherwise accurate studies of A23187-induced cell death prevents both a comparison with the present results, and an assessment of the relative role of cPLA$_2$ activation and cytosolic Ca^{2+} overload in determining cell death in other models. It must be stressed that an adequate kinetic resolution of the ionophore-induced $[Ca^{2+}]_c$ changes is essential to substantiate a cause-effect relationship with the subsequent cellular changes. Indeed, and consistent with the findings of Gwag *et al.* (30), we observed a delayed rise of $[Ca^{2+}]_c$ after the addition of A23187 that could be largely prevented by aristolochic acid, indicating that the $[Ca^{2+}]_c$ rise was the consequence rather than the cause of mitochondrial dysfunction (results not shown).

Previous studies have related the mode of cell death to the ionophore concentration; low concentrations causing apoptosis and higher concentrations causing necrosis in cultured cortical neurons and PC12 cells (30, 31). In our system increasing the A23187 concentration from 2 to 5 μM did not change the profile of the $[Ca^{2+}]_c$ transient or the pattern of cell death, and quite similar results were obtained if ionomycin was used (results not shown). It appears that the response to ionophores may be somewhat different depending on the cell type. Yet, our findings document a key role of cPLA$_2$ and arachidonic acid release as the initiator events of the apoptotic cascade in protocols based on the addition of A23187. Whether cytosolic Ca^{2+} overload can bypass the otherwise necessary activation of cPLA$_2$ is under active investigation in our laboratories.

REFERENCES

1. Shen, A. C., and Jennings, R. B. (1972) *Am. J. Pathol.* **67,** 417–440
2. Fleckenstein, A., Janke, J., Doring, H. J., and Leder, O. (1974) *Rec. Adv. Stud. Cardiac. Struct. Metab.* **4,** 563–580
3. Orrenius, S., Zhivotovsky, B., and Nicotera, P. (2003) *Nat. Rev. Mol. Cell. Biol.* **4,** 552–565
4. Rizzuto, R., Bernardi, P., and Pozzan, T. (2000) *J. Physiol. (Lond.)* **529,** 37–47
5. Bernardi, P. (1999) *Physiol. Rev.* **79,** 1127–1155
6. Bernardi, P., Petronilli, V., Di Lisa, F., and Forte, M. (2001) *Trends Biochem. Sci.* **26,** 112–117
7. Scorrano, L., Ashiya, M., Buttle, K., Weiler, S., Oakes, S. A., Mannella, C. A., and Korsmeyer, S. J. (2002) *Dev. Cell* **2,** 55–67
8. Petronilli, V., Miotto, G., Canton, M., Colonna, R., Bernardi, P., and Di Lisa, F. (1999) *Biophys. J.* **76,** 725–734
9. Petronilli, V., Penzo, D., Scorrano, L., Bernardi, P., and Di Lisa F. (2001) *J. Biol. Chem.* **276,** 12030–12034
10. Nicolli, A., Petronilli, V., and Bernardi, P. (1993) *Biochemistry* **32,** 4461–4465
11. Arora, A. S., Jones, B. J., Patel, T. C., Bronk, S. F., and Gores, G. J. (1997) *Hepatology* **25,** 958–963
12. Pacher, P., and Hajnoczky, G. (2001) *EMBO J.* **20,** 4107–4121
13. Scorrano, L., Petronilli, V., Di Lisa, F., and Bernardi, P. (1999) *J. Biol. Chem.* **274,** 22581–22585
14. Rippo, M. R., Malisan, F., Ravagnan, L., Tomassini, B., Condo, I., Costantini, P., Susin, S. A., Rufini, A., Todaro, M., Kroemer, G., and Testi, R. (2000) *FASEB J.* **14,** 2047–2054
15. Garcia-Ruiz, C., Colell, A., Paris, R., and Fernandez-Checa, J. C. (2000) *FASEB J.* **14,** 847–858
16. Kristal, B. S., and Brown, A. M. (1999) *J. Biol. Chem.* **274,** 23169–23175
17. Scorrano, L., Penzo, D., Petronilli, V., Pagano, F., and Bernardi, P. (2001) *J. Biol. Chem.* **276,** 12035–12040
18. Gugliucci, A., Ranzato, L., Scorrano, L., Colonna, R., Petronilli, V., Cusan, C., Prato, M., Mancini, M., Pagano, F., and Bernardi, P. (2002) *J. Biol. Chem.* **277,** 31789–31795
19. Penzo, D., Tagliapietra, C., Colonna, R., Petronilli, V., and Bernardi, P. (2002) *Biochim. Biophys. Acta Bioenerg.* **1555,** 160–165
20. Hayakawa, M., Ishida, N., Takeuchi, K., Shibamoto, S., Hori, T., Oku, N., Ito, F., and Tsujimoto, M. (1993) *J. Biol. Chem.* **268,** 11290–11295
21. Pastorino, J. G., Simbula, G., Yamamoto, K., Glascott, P. A. Jr., Rothman, R. J., and Farber, J. L. (1996) *J. Biol. Chem.* **271,** 29792–29798
22. Chan, T. A., Morin, P. J., Vogelstein, B., and Kinzler, K. W. (1998) *Proc. Natl. Acad. Sci. U. S. A.* **95,** 681–686
23. Cao, Y., Pearman, A. T., Zimmerman, G. A., McIntyre, T. M., and Prescott, S. M. (2000) *Proc. Natl. Acad. Sci. U. S. A.* **97,** 11280–11285
24. Simbula, G., Glascott, P. A., Jr., Akita, S., Hoek, J. B., and Farber, J. L. (1997) *Am. J. Physiol.* **273,** C479-C488
25. Michel, P. P., Vyas, S., Anglade, P., Ruberg, M., and Agid, Y. (1994) *Eur. J. Neurosci.* **6,** 577–586
26. Mattson, M. P., Rychlik, B., Chu, C., and Christakos, S. (1991) *Neuron* **6,** 41–51
27. Lukas, W., and Jones, K. A. (1994) *Neuroscience* **61,** 307–316
28. Qian, T., Herman, B., and Lemasters, J. J. (1999) *Toxicol. Appl. Pharmacol.* **154,** 117–125
29. Petersen, A., Castilho, R. F., Hansson, O., Wieloch, T., and Brundin, P. (2000) *Brain Res.* **857,** 20–29
30. Gwag, B. J., Canzoniero, L. M., Sensi, S. L., Demaro, J. A., Koh, J. Y., Goldberg, M. P., Jacquin, M., and Choi, D. W. (1999) *Neuroscience* **90,** 1339–1348
31. Takadera, T., and Ohyashiki, T. (1997) *Eur. J. Biochem.* **249,** 8–12
32. Bernardi, P., Scorrano, L., Colonna, R., Petronilli, V., and Di Lisa F. (1999) *Eur. J. Biochem.* **264,** 687–701
33. Bligh, E. G., and Dyer, W. J. (1959) *Can. J. Biochem. Physiol.* **37,** 911–917
34. Gijon, M. A., and Leslie, C. C. (1999) *J. Leukoc. Biol.* **65,** 330–336
35. Hirabayashi, T., and Shimizu, T. (2000) *Biochim. Biophys. Acta* **1488,** 124–138
36. Grewal, S., Ponnambalam, S., and Walker, J. H. (2003) *J. Cell Sci.* **116,** 2303–2310
37. Pouliot, M., McDonald, P. P., Krump, E., Mancini, J. A., McColl, S. R., Weech, P. K., and Borgeat, P. (1996) *Eur. J. Biochem.* **238,** 250–258
38. Chandra, V., Jasti, J., Kaur, P., Srinivasan, A., Betzel, C., and Singh, T. P. (2002) *Biochemistry* **41,** 10914–10919
39. Vishwanath, B. S., Fawzy, A. A., and Franson, R. C. (1988) *Inflammation* **12,** 549–561
40. Rosenthal, M. D., Vishwanath, B. S., and Franson, R. C. (1989) *Biochim. Biophys. Acta* **1001,** 1–8
41. Reed, P. W., and Lardy, H. A. (1972) *J. Biol. Chem.* **247,** 6970–6977
42. Pfeiffer, D. R., and Lardy, H. A. (1976) *Biochemistry* **15,** 935–943
43. Dordick, R. S., Brierley, G. P., and Garlid, K. D. (1980) *J. Biol. Chem.* **255,** 10299–10305
44. Babcock, D. F., First, N. L., and Lardy, H. A. (1976) *J. Biol. Chem.* **251,** 3881–3886
45. Pickett, W. C., Jesse, R. L., and Cohen, P. (1976) *Biochim. Biophys. Acta* **486,** 209–213
46. Borgeat, P., and Samuelsson, B. (1979) *Proc. Natl. Acad. Sci. U. S. A.* **76,** 2148–2152
47. Jayadev, S., Linardic, C. M., and Hannun, Y. A. (1994) *J. Biol. Chem.* **269,** 5757–5763
48. Jayadev, S., Hayter, H. L., Andrieu, N., Gamard, C. J., Liu, B., Balu, R., Hayakawa, M., Ito, F., and Hannun, Y. A. (1997) *J. Biol. Chem.* **272,** 17196–17203
49. Garcia-Ruiz, C., Colell, A., Mari, M., Morales, A., and Fernandez-Checa, J. C. (1997) *J. Biol. Chem.* **272,** 11369–11377
50. Garcia-Ruiz, C., Colell, A., Morales, A., Calvo, M., Enrich, C., and Fernandez-Checa, J. C. (2002) *J. Biol. Chem.* **277,** 36443–36448
51. Garcia-Ruiz, C., Colell, A., Mari, M., Morales, A., Calvo, M., Enrich, C., and Fernandez-Checa, J. C. (2003) *J. Clin. Investig.* **111,** 197–208
52. De Maria, R., Lenti, L., Malisan, F., d'Agostino, F., Tomassini, B., Zeuner, A., Rippo, M. R., and Testi, R. (1997) *Science* **277,** 1652–1655